ISSN 1027-5495. Functional Materials, 29, No.4 (2022), p. 605-610.
doi:https://doi.org/10.15407/fm29.04.605

Utilization of kaolinite to synthesize NaP zeolite for dye wastewater removal

***Xuefeng Yuan*[1], *Gang Liao*[2]**

[1]Taizhou Polytechnical College, Jiangsu Taizhou 225300, China
[2]Department of Traffic and Municipal Engineering, Sichuan College of Architectural Technology, 610399 Sichuan Chengdu, China

Received September 28, 2022

In this paper, kaolinite was used to synthesize zeolite by using a hydrothermal method. Before synthesis, kaolinite was pre-treated by alkali-fusion. The as-prepared zeolite was used to remove MB in wastewater. The effect of synthesis condition (including NaOH/Kaolinite mass ratio, activation temperature, and hydrothermal temperature) on the adsorption capacity and MB removal efficiency. The microstructure of zeolite was characterized by X-ray diffraction,scanning electron microscopy (SEM) and N_2 adsorption-desorption tests. Various adsorption kinetic models were used to elucidate the adsorption process and acquire the adsorption rate constant. The results show that zeolite was sphere-like and had a mesopore structure. The adsorption capacity was about 34.06 mg/g. This as-synthesized zeolite was an excellent purification material for removing dye wastewater.
Keywords: kaolinite, NaP zeolite, dye wastewater, adsorption capacity.

Використання каолініту для синтезу NaP-цеоліту для очищення стічних вод від барвників. *Xuefeng Yuan, Gang Liao*

В роботі використано каолініт для синтезу цеоліту за допомогою гідротермального методу. Перед синтезом каолініт було попередньо оброблено сплавленням з лугом. Отриманий цеоліт було використано для видалення барвника метиленового блакитного зі стічних вод. Визначено вплив умов синтезу (включно із масовим співвідношенням NaOH/каолініт, температурою активації та гідротермальною температурою) на адсорбційну здатність та ефективність видалення барвника. Мікроструктуру цеоліту характеризовано рентгенівською дифракцією, скануючою електронною мікроскопією та тестом на адсорбцію-десорбцію азоту. Для висвітлення процесу адсорбції використано різні кінетичні моделі. Показано, що отриманий цеоліт має сфероподібну мезопористу структуру. Адсорбційна здатність складала близько 34,06 мг/g. Синтезований таким чином цеоліт може бути відмінним очисним матеріалом для видалення барвників із стічних вод.

1.Introduction

Dye stuff is an indispensable material in modern society, which is widely used in our life [1–2]. However, with the immoderate discharge of dye wastewater into aquatic environment, the water resource is severely contaminated. Moreover, the dye stuff is non-biodegradable and very stable in water. The dye wastewater has caused serious ecological problems in some districts, such as the disappearance of aquatic animals or plants [3–4]. People have carried out many methods to purify dye wastewater, such as photocatalytic degradation, physical adsorption, chemical oxidation, electric catalytic degradation et al. [5–7]. Although these methods are effective in eliminating dye wastewater, most of them can't be applied in large scale due to the high cost and complicated operation. Adsorption is considered as the most promising technology in dye wastewater removal, because it's easily applied and cost-effective [8, 9].

There are many materials used for adsorption of dye stuff in wastewater, such as active carbon, zeolite, diatomite, attapulgite, et al. Zeolite has mesostructure pores and ion exchange capacity, especially for cations, exhibiting excellent adsorption capacity [10–11]. Therefore, zeolite is widely used in environmental remediation. However, in the last few decades, pure chemical reagents were used to synthesize zeolite, which increased the cost of zeolite and limited the use of zeolite [12]. In order to reduce the cost of zeolite, some inexpensive natural minerals are used to synthesize zeolite. Kaolinite is an ordinary natural mineral containing large amounts of SiO_2 and Al_2O_3, which is suitable to synthesize zeolite [13]. The synthesis process of zeolite mainly contains alkali activation, digestion of Si or Al, nucleation, and crystallization. Hydrothermal treatment is the widely used method to synthesize zeolite.

In this paper, kaolinite was used as a raw material to synthesize P zeolite (PZ), and the as-prepared PZ was used in dye wastewater treatment. The methylene blue (MB) solution was selected to simulate the dye wastewater. The effect of synthesis parameters on the adsorption efficiency of PZ was investigated systemically. The microstructure of PZ was characterized by X-ray diffraction (XRD), scanning electron microscopy (SEM) and N_2 adsorption-desorption tests. Our work may promote the application of zeolite in dye wastewater purification.

2. Materials and method

2.1. Materials

Kaolinite was derived from Zhejiang province of China. The kaolinite was ground in a ball mill and sieved through a 200 mesh. NaOH was provided by Sinopharm Chemical Reagent Co., Ltd.

Table 1. Synthesis conditions of zeolite

No.	Alkali/ kaolinite ratio	Activation temperature, °C	Hydrothermal temperature, °C
Z1	0.8	550	120
Z2	1	550	120
Z3	1.2	550	120
Z4	1.4	550	120
Z5	1.2	550	80
Z6	1.2	550	100
Z7	1.2	550	140
Z8	1.2	350	120
Z9	1.2	450	120
Z10	1.2	650	120

2.2. Zeolite synthesis

5 g of kaolinite and a proper amount of NaOH were mixed and calcinated at 550°C for 2 h. The sintered product was ground and mixed with some water, and stirred and sonicated for 30 min. The suspension was added to a teflon liner and treated in a stainless steel kettle at 120°C for 12 h. To investigate the effect of synthesis conditions on the property of zeolite, alkali addition, activation temperature, and hydrothermal temperature were varied and various samples were prepared as shown in Table 1.

2.3. Characterization

X-ray diffraction was used to characterize crystal phases of samples. The X-ray diffraction (XRD) patterns of samples were recorded in Cu–Kα radiation using an advanced diffractometer (D/max2550, RIGAKU, Japan) equipped with a fast position sensitive detector. The micro-morphology of samples was observed on a scanning electron microscope (TM400Plus, HITACHI, Japan). To characterize the surface area and pore structure of samples, the N_2 adsorption-desorption test was carried out using a surface area automatic analyzer (3H-2000PS2, BEISHIDE, China).

2.4. MB removal experiment

The concentration of the MB solution was fixed at 10 mg/L. 25 mg of the sample and 100 mL of the MB solution were added to a conical flask and placed in an oscillating bed at a constant temperature of 25°C for 2 h. Subsequently, 5 ml of the suspension was fetched and centrifugated for 5 min, and then the absorbance of the supernatant was measured. Then, the concentration of the MB solution was calculated according the Beer-Lambert law. The adsorption capacity of zeolite can be calculated as:

$$\xi = \frac{(C_0 - C_e) \cdot V}{m_z}. \quad (1)$$

The MB removal efficiency can be calculated as:

$$\varphi = 1 - \frac{C_e}{C_0}. \quad (2)$$

To describe the adsorption process, various adsorption kinetic models were used to fit the adsorption data. The pseudo-first-order model, the pseudo-second-order

model, and the intraparticle diffusion model are described by Eq. (3)–(5), respectively.

$$Ln(q_e - q_t) = Lnq_e - k_1 t, \quad (3)$$

$$\frac{t}{q_t} = \frac{1}{(k_2 q_e^2)} + \frac{1}{q^e} t. \quad (4)$$

$$q_t = k_i t^{0.5} + c, \quad (5)$$

where q_e and q_t are the adsorbed quantity of MB at equilibrium and t (min) time, respectively; k_1, k_2, k_i are the adsorption rate constants for the three models, respectively; C is a constant characterizing the thickness of the boundary layer.

3. Results and discussion

3.1. Microstructure of zeolite

Fig. 1 shows the X-ray diffraction patterns of kaolinite, alkali-treated product, and as-prepared zeolite. There are strong diffraction peaks of quartz in the kaolinite diffraction pattern, indicating that kaolinite was not pure and contained some quartz. Due to the high inertness of quartz, it is difficult to activate it, which is unfavorable to the formation of zeolite. Therefore, high-temperature treatment is required to activate kaolinite. As shown in the diffraction pattern of the alkali-treated intermediate product, the diffraction peaks of quartz and kaolinite disappeared after calcination at 550°C, indicating that the crystal structure of kaolinite and quartz were destroyed. Na_2O reacted with Si–O tetrahedron and Al–O tetrahedron, thus forming Na_2SiO_3 and $NaAlO_2$. Thus, the diffraction peaks of Na_2SiO_3 can be observed in the intermediate product. After hydrothermal treatment, the characteristic diffraction peaks of NaP zeolite appeared, indicating the formation of NaP zeolite. NaP zeolite has a GIS topological structure and a microporous structure. The interlaced eight-ring formed pore channels 0.31–0.44 nm in size in the [100] lattice plane and 0.26–0.49 nm in the [010] lattice plane [14].

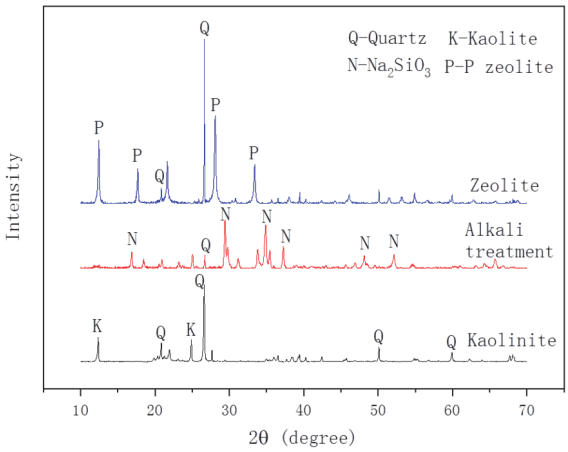

Fig. 1. X-ray diffraction patterns of kaolinite, alkali-treated intermediate product, and zeolite.

Fig. 2 presents the micro-morphology of kaolinite and as-prepared NaP zeolite. It can be seen that kaolinite was stacked of plate-like units. And the NaP zeolite displayed the typical sphere structure. The diameter of a zeolite microsphere was about 3 μm, and these microspheres were uniform. In addition, the zeolite surface was covered with some flocculent substance, which may be the precursor of NaP zeolite.

Fig. 3(a) exhibits the N_2 adsorption-desorption isotherms of kaolinite and zeolite, which belong to the ? type isotherm.

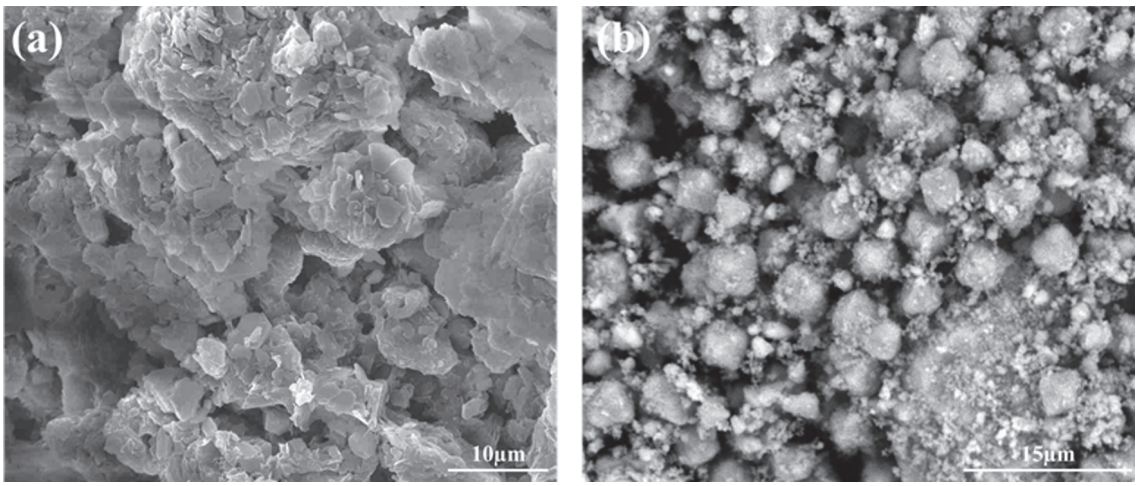

Fig. 2. Micro-morphology of (a) kaolinite and (b) NaP zeolite.

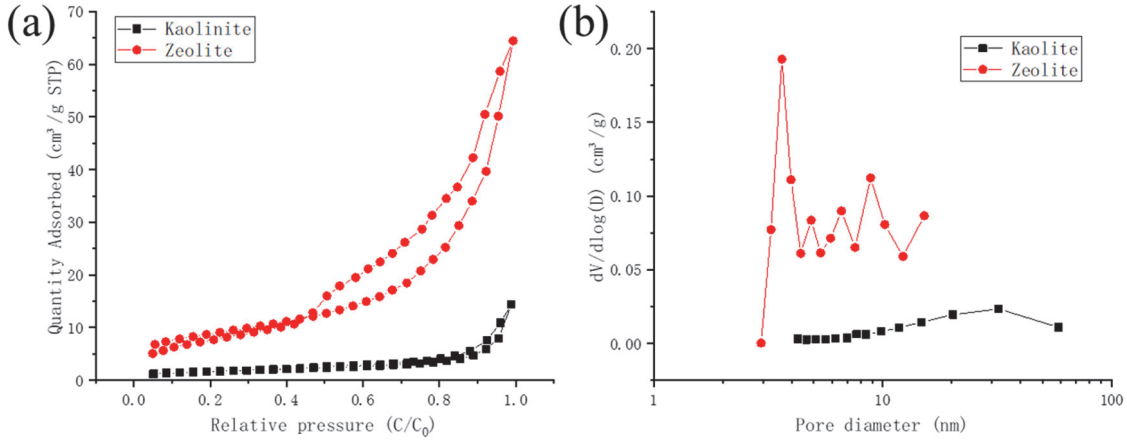

Fig. 3. (a) N_2 adsorption-desorption isotherms, (b) pore size distribution of kaolinite and zeolite.

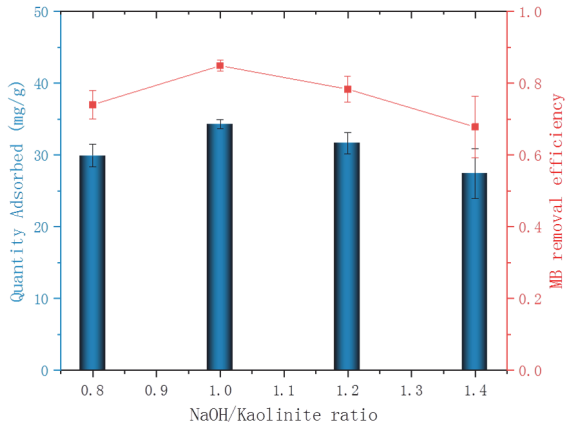

Fig. 4. Effect of the NaOH/kaolinite ratio on the adsorption capacity and MB removal efficiency.

An H3 type hysteresis loop was observed in the isotherms, which was caused by a stack of sphere-like zeolite particles. The adsorbed amount of kaolinite was very low, indicating the low content of mesopores and the high content of macro-pores, which was also confirmed by the SEM image of kaolinite. However, the adsorbed amount of zeolite was much higher than that of kaolinite, indicating a higher porosity of zeolite. As the relative pressure increases, the amount of adsorption gradually increases, and hysteresis loop appears at the medium relative pressure, which is a typical characteristic of mesoporous materials. In addition, the BET surface area of zeolite (30.9417 g/m^2) was higher than that of kaolinite (6.12083 g/m^2) as shown in Table 2. Fig. 3(b) shows the pore size distribution curve of zeolite, which confirmed the mesoporous distribution characteristics. And the most probable pore size of zeolite particles was about 4 nm. According to the

Table 2. Surface area, pore volume, and pore size of kaolinite and zeolite

No.	S_{BET}, g/m^2	Pore Volume, cm^3/g	Pore Size, nm
Kaolinite	6.12083	0.021537	14.8614
Zeolite	30.9417	0.064654	9.2384

classification of the International Union of Pure and Applied Chemistry (IUPAC), this type of hysteresis loop belongs to type H5. The pore structure of zeolite is suitable for adsorption of contaminants.

3.2. MB removal performance

Fig. 4 shows the effect of NaOH/kaolinite mass ratio on the MB removal efficiency and adsorption capacity of as-prepared samples. As the amount of NaOH increases, the adsorption capacity and MB removal efficiency improve; and at NaOH/kaolinite mass ratio of 1.0, zeolite had the highest adsorption capacity and MB removal efficiency, reaching 34.27 mg/g and 84.86 %, respectively. After exceeding 1.0, the adsorption capacity decreased with an increase in the NaOH/kaolinite mass ratio. This is due to the transformation of the mineral phase at different NaOH concentrations. With a small addition of NaOH, neither partial kaolinite nor quartz was activated by Na_2O and its Si–O tetrahedron was stable; thus, there was some inactive substance in the final product. At a high NaOH concentration, NaP was easy to transform to sodalite, which has a smaller pore size and low porosity. Sodalite has a microporous structure, and the length of the main chain of the MB molecule was about 1.447 nm, therefore, most MBs cannot access the micropores.

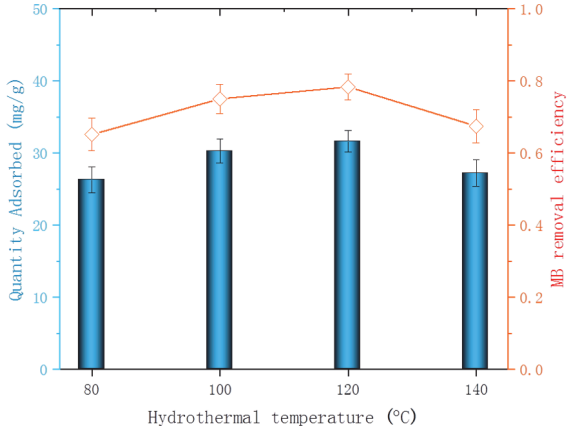

Fig. 5. Effect of hydrothermal temperature on the adsorption capacity and MB removal efficiency.

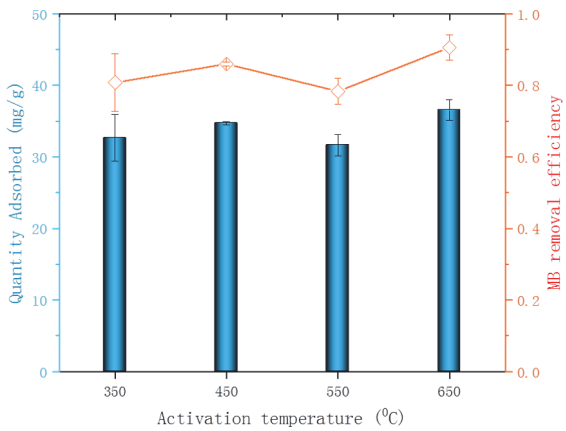

Fig. 6. Effect of activation temperature on the adsorption capacity and MB removal efficiency.

As shown in Fig. 5, the adsorption capacity and MB removal efficiency increased with hydrothermal temperature, and the sample treated at 120°C had the highest adsorption ability. After exceeding 120°C, the adsorption capacity of as-prepared sample decreased obviously. This can be explained by the fact, that under low temperature, the precursor of NaP zeolite can overcome the energy barrier of zeolite crystallization, a small amount of NaP zeolite is formed; however, under high temperature, the formed NaP zeolite is easily converted into sodalite.

Fig. 6 displays the effect of activation temperature on the adsorption capacity and MB removal efficiency. Generally, the adsorption capacity and MB removal efficiency increased with the activation temperature. The sample treated at 650°C exhibited the highest adsorption capacity (36.56 mg/g) and MB removal efficiency (90.54 %). Since the melting and boiling points of NaOH were 318°C and 1388°C, in theory NaOH will react with kaolinite in the range of 318°C to 1388°C. But when temperature was lower, NaOH didn't melt absolutely. In addition, higher temperature accelerated the NaOH mass transfer; thus, more Si–O or Al–O bonds were broken, generating more active precursor for zeolite synthesis.

3.3. Adsorption kinetics

Fig. 7(a) shows that as-synthesized NaP zeolite has a high adsorption rate towards MB, and over a half of the MB can be adsorbed by zeolite within the first 5 min. Moreover, 90 % of the equilibrium absorption can be achieved within 30 min. The amount of the adsorbed substance gradually increased with the contact time and reached the adsorption equilibrium within 2 h. The fitting goodness (R^2) of the pseudo-second-order kinetic model was the highest, reaching 0.99856, while R^2 of the other two models were 0.88628 and 0.76392, respectively, indicating the adsorption process may follow the second-order kinetic model. The theoretical adsorbed amount of zeolite for MB removal calculated from the pseudo-second-order model is 36.07 mg/g, which is close to the experimental value (34.07 mg/g), indicating that the MB adsorption onto zeolite may be determined by the availability of adsorption sites.

4. Conclusions

NaP zeolite was successfully synthesized using kaolinite as a raw material. The most optimal synthesis conditions were the following: the NaOH/kaolinite mass ratio of 1, activation temperature of 650°C, hydrothermal temperature of 120°C. The as-prepared zeolite consisted of sphere-like particles with the diameter of 3 μm and had a mesopore structure and a high specific surface area. Zeolite exhibited a high adsorption capacity towards MB, and the equilibrium adsorbed amount of MB can reach 34.06 mg/g. The adsorption process corresponded to the pseudo-second-order model. Moreover, the adsorption speed was fast and 80 % equilibrium adsorbed amount could be achieved within 30 min. The as-prepared zeolite was an ideal adsorption material for purification of dye wastewater.

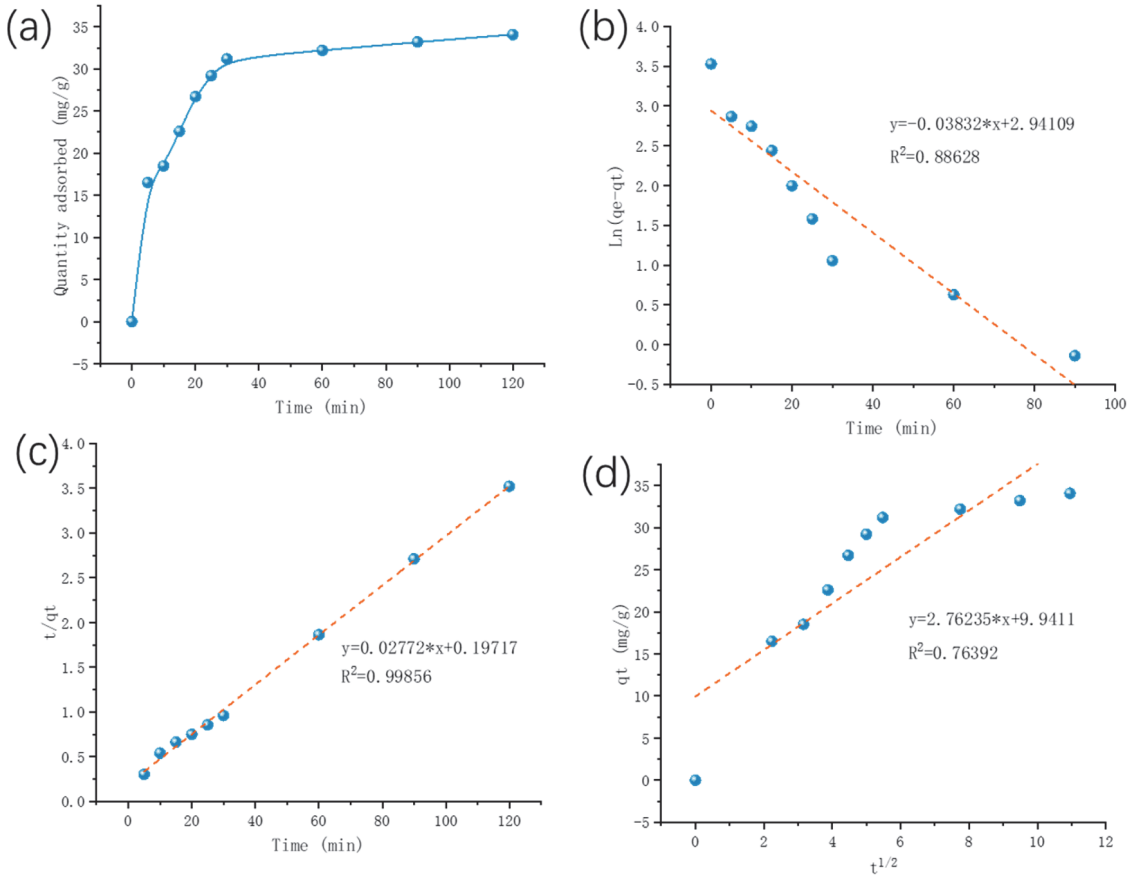

Fig. 7. (a) Time-dependent adsorption capacity of PZ the and linear fitting of the (b) pseudo-first-order, (c) pseudo-second-order, and (d) intraparticle diffusion models.

References

1. S.Ahmed, M.G.Rasul, W.N.Martens et al., *Water, Air, & Soil Pollution*, **215**, 3 (2011).
2. R.O.Alves de Lima, A.P.Bazo, D.M.F.Salvadori et al., *Mutation Research/Genetic Toxicology and Environmental Mutagenesis*, **626**, 53 (2007).
3. R.Adnan, I.Shah, *Environmental Science and Pollution Research*, **23**, 15941 (2016).
4. M.T.Amin, A.A.Alazba, U.Manzoor, *Advances in Materials Science and Engineering*, 825910 (2014).
5. L.Jiang, X.Yuan, Y.Pan et al., *Applied Catalysis B: Environmental*, **217**, 388 (2017).
6. J.Zhang, M.Yan, G.Sun, K.Liu, *Sep. Purif. Technol.*, **272**, 118888 (2021).
7. H.Zangeneh, A.Zinatizadeh, M.Habibi et al., *Journal of Industrial and Engineering Chemistry*, **26**, 1 (2015).
8. M.R.Gadekar, M.M.Ahammed, *Journal of Environmental Management*, **231**, 241 (2019).
9. I.Jansson, S.Suarez, F.J.Garcia-Garcia, B.Sanchez, *Applied Catalysis B: Environmental*, **178**, 100 (2015).
10. A.Corma, H.Garcia, *Chem. Commun.*, 1443 (2004).
11. S.-H.Liu, W.-X. Lin, *J. Hazard. Mater.*, **368**, 468 (2019).
12. X.Pu, L.Yao, L.Yang et al., *Journal of Cleaner Production*, **265**, 121822 (2020).
13. W.Khanday, F.Marrakchi, M.Asif, B.Hameed, *Journal of the Taiwan Institute of Chemical Engineers*, **70**, 32 (2017).
14. P.Sharma, J.-g.Yeo, M.H.Han, C.H.Cho, *Journal of Materials Chemistry A*, **1**, 2602 (2013).